

ASSESSING AND MANAGING EARTHQUAKE RISK

Editors: C.S. Oliveira, A. Roca and X. Goula

Springer Verlag

ISBN 10-1-4020-3524-1

Páginas 115-134

CHAPTER 6 VULNERABILITY ASSESSMENT OF DWELLING BUILDINGS

A.H. Barbat¹, S. Lagomarsino² and L.G. Pujades¹

1. *Universitat Politècnica de Catalunya, Barcelona, Spain*

2. *University of Genoa, Genoa, Italy*

6.1. Introduction

Risk is defined as the potential economic, social and environmental consequences of hazardous events that may occur in a specified area unit and period of time. Its estimation requires a multidisciplinary approach that takes into account not only the expected physical damage understood as the damage suffered by structures, the number and type of casualties or the economic losses, but also social, organizational and institutional factors. At urban level, for example, vulnerability should be also related to the social fragility and the lack of resilience of the exposed community, that is, to its capacity to absorb the impact and control its implications. Nevertheless, a holistic approach to estimate risk aiming to guide the decision making at urban level should start with the evaluation of physical damage scenarios as an essential tool, because they are the result of the convolution between hazard and physical vulnerability for buildings and infrastructure (Cardona 2001; Barbat 2003). Accordingly, the evaluation of physical vulnerability and risk of buildings is the main purpose of this chapter. Some definitions related to these concepts are introduced here below.

Risk, $Rie|_T$, can be defined as the probability of loss in an exposed element e as a consequence of the occurrence of an event with intensity larger than or equal to i during an exposition period T .

Hazard, $Hi|_T$, can be understood as the probability of occurrence of an event with an intensity greater than or equal to i during an exposition period T .

Vulnerability, Ve , is the intrinsic predisposition of the exposed element e to be affected or of being susceptible to suffer a loss as a result of the occurrence of an event with intensity i .

Starting from these definitions, risk is a function f of the convolution between hazard Hi and vulnerability Ve during an exposition period T

$$Rie|_T = f(Hi \otimes Ve)|_T \quad (6.1)$$

where the symbol \otimes stays for convolution (Cardona and Barbat 2000).

The major part of losses due to earthquakes has its origin in the deficient seismic behaviour of structures. In spite of the advances of research in earthquake engineering in general and particularly on seismic design codes, catastrophic losses have occurred recently in many countries in the world, including countries in which earthquake engineering studies are priority tasks. It is clear that new developments in earthquake resistant design can only be applied to new projects, which represent a small part of the existing structures in a seismic area. Therefore, the only possibility of reducing earthquake losses is improvement of the seismic behaviour of existing structures. The aim of risk studies is to predict the expected damage in structures due to a specified earthquake. A seismic risk analysis addressed to earthquake emergency management and protection strategies planning, requires territorial scale evaluation. Once the expected damage is predicted, it is possible to find solutions to diminish it, which rebound in the cost of the structures; this cost can be compared with the expected losses, in order to decide if structural retrofit or structural reinforcement are feasible. In spite of

the importance of this type of studies, standard methodologies to estimate the vulnerability of structures are not available.

6.2. Methodologies for vulnerability assessment

Dolce et al. (1994) classified methodologies for the evaluation of structural vulnerability in four groups: (a) direct, which assesses in a simple way the damage caused in a structure by a given earthquake; (b) indirect, which determines first a vulnerability index of the structure and then assesses the relationship between damage and seismic intensity; (c) conventional, which is essentially a heuristic method, introducing a vulnerability index independent of the damage prediction; (d) hybrid, which combines elements of the previous methods with expert judgments. The selection of one of these methods depends on the objectives of the study, the type of the results required and on the available information. On the other hand, fragility functions, damage probability matrices and vulnerability functions obtained from observed structural damages during past earthquakes in a seismic area were the preferred tools in seismic risk studies performed in the past (Kappos et al. 1995; Benedetti and Petrini 1984; Barbat et al. 1996).

The damage probability matrices and vulnerability functions are defined in the following way: 1) Damage Probability Matrices (DPM) express in a discrete form the conditional probability $P[D = j|i]$ to obtain a damage level j , due to an earthquake of severity i (Whitman 1974); and 2) Vulnerability Functions are relations expressing the vulnerability in a continuous form, as functions of certain parameters that describe the size of the earthquake (Benedetti and Petrini 1984). The vulnerability assessment is performed in terms of qualitative parameters: buildings are classified in vulnerability classes, and a DPM is assigned to each class or, alternatively, scores are attributed to the buildings considering their typological, structural, geometric and constructive characteristics; a simple model is then defined as a function of the evaluated scores relating the seismic input to the expected damage (Benedetti and Petrini, 1984; FEMA, 1998).

A complete observed damage data base would be desirable for applying such approaches; however, this is only possible in certain high seismicity areas where post-earthquake survey studies have been properly performed. Where the information is limited, damage matrices and vulnerability functions can be established using the available data and local expert opinion (Anagnos et al. 1995). Finally, in countries without any available damage data base, the information obtained in other similar areas is applied in a direct (Chavez and García-Rubio 1995) or modified form, using expert judgment (Bustamante et al. 1995). Some authors have used hybrid methodologies to assess the vulnerability of buildings (Chavez and García-Rubio 1995), developing fragility curves and damage probability matrices in order to estimate the feasibility of seismic rehabilitation of existing reinforced concrete (RC) buildings.

As the available data are often incomplete and do not concern all the building typologies and all the intensities that would be necessary to be represented in a model, probabilistic processing of the observed data is supported or completely replaced by other approaches such as structural analysis methods (Milutinovic and Trendafiloski 2003), expert judgement (ATC-13, 1985), neural network systems (Dong et al. 1988) or fuzzy set theory (Sanchez-Silva and Garcia 2001). To complete the undesirable lack of earthquake damage information in an area, simulation procedures can be also applied. The probabilistic analysis of computer generated structural responses obtained by using complex or simplified models and nonlinear analysis procedures of representative buildings can provide fragility curves, damage probability matrices and vulnerability functions relating seismic intensity or peak ground acceleration with damage (Noceviski

and Petrovski, 1994; Kappos et al., 1995; Singhal and Kiremidjian, 1996). In these studies, the damage estimated for a generic structure pertaining to a given typology is considered as representative for the whole range of structures belonging to the mentioned structural typology.

In the vulnerability index method, the study is extended to a large number of classes of buildings within each of the considered typologies; these classes are defined through parameters which cover most of the structural characteristics, aiming to discriminate among different seismic behaviours of buildings with the same structural typology located in a specified seismic area (Benedetti and Petrini, 1984). This method, based on a great amount of damage survey data corresponding to several seismic zones of Italy, identifies the most important eleven parameters controlling the damage in buildings caused by earthquakes and qualifies them individually by means of qualification coefficients K_i , affected by weights W_i , which try to emphasize their relative importance. The method makes an overall qualification of the buildings by means of a vulnerability index I_v . Thus, the global vulnerability index of each building is evaluated by means of the formula

$$I_v = \sum_{i=1}^{11} K_i \times W_i \quad (6.2)$$

Using vulnerability functions, it is possible to relate I_v with an overall damage index D of the buildings, whose values, expressed as a percentage, also range between 0 and 100. The eleven mentioned parameters are: structural system organization, structural system quality, conventional strength, retaining walls and foundation, floor system, configuration in plant, configuration in elevation, maximum distance between walls, roof type, non-structural elements and preservation state.

An economic damage index corresponding to the physical risk of buildings could be defined as the relation between the damage repair cost and reposition cost. Both in the case of unreinforced masonry buildings and reinforced concrete buildings it is not reasonable to consider the overall structural damage index equal to the economic damage index (which includes the cost of non-structural elements (furniture, equipment, installations, etc.) which usually contribute to the major part of the economic losses (Gunturi, 1993).

A damage index can be obtained for each structural component of a reinforced concrete building. Then it is possible to evaluate an economic damage index for each floor $D_{ec,k}$ by means of the equation

$$D_{ec,k} = \frac{\sum D_{ec,i} \times w_i}{\sum w_i} \quad (6.3)$$

where $D_{ec,i}$ is the structural damage index for each element i of floor k and w_i is the reposition cost of this element. The economic damage index of the entire structure can be then obtained as the average of all the structural floor indices. The economic floor damage index for architectural elements and equipment can be also evaluated starting from the maximum drifts and accelerations of floors obtained from a nonlinear analysis of the structures. Finally, the global economic damage index of the building can be obtained as a weighted average of the economic structural and non-structural economic damage indices.

In the United States, and nowadays also in Europe, the most recent trends in the field of vulnerability evaluation for risk analysis operate with simplified mechanical models,

essentially based on the Capacity Spectrum Method (Freeman, 1998b; NIBS, 1997, 1999 and 2002). This method permits evaluating the expected seismic performance of structures by comparing, in spectral coordinates (S_d , S_a), their seismic capacity with the seismic demand, described by Acceleration-Displacement Response Spectra (ADRS) adequately reduced in order to take into account the inelastic behaviour (Fajfar, 2000). For purposes of territorial vulnerability assessment, capacity spectrum procedures do not necessarily use capacity curves obtained by pushover analyses, but they ascribe bilinear capacity curves defined by yielding (D_y , A_y) and ultimate (D_u , A_u) capacity points to each building typology; these curves vary depending on geometrical and technological parameters, characteristic of the buildings (number of floors, code level, material strength, drift capacity, etc.). Such an approach provides reliable results if applied to a built-up area characterized by a typological building homogeneity and by consolidated seismic design codes. This is not the case in the European Union where seismic codes are very different and where various typologies of masonry buildings can be distinguished in the territory. In this case, the employment of capacity based methods needs, yet, a robust experimental validation, at least on the traditional masonry constructions; for this reason, statistical methods based on damage observations are required.

A method derived in a theoretically rigorous way, starting from EMS-98 macroseismic scale (Grünthal, 1998) definitions overcomes the distinction between typological and rating methods and allows carrying out a vulnerability analysis with a single approach, graded to different levels according to the quantity and quality of the available data and the size of the territory. The method, which is applicable to all the European regions, has been verified on the basis of data observed after earthquakes occurred in different countries. The vulnerability index method in its version mentioned before and the capacity spectrum method are described in detail in the following sections of this chapter.

6.3. Vulnerability index method based on the EMS-98 macroseismic scale

6.3.1. EMS-98 BASED VULNERABILITY CURVES

6.3.1.1. Vulnerability model implicitly contained in the EMS-98 scale

The aim of a macroseismic scale is to measure the earthquake severity starting from the observation of the damage suffered by buildings and therefore it represents, for forecast purposes, a vulnerability model able to supply, for a given intensity, the probable damage distribution. In this sense, the EMS-98 scale, which will probably be used in the future at European level, contains a clear and detailed definition of the different building typologies and a precise description of the degrees of damage and of the damage distribution related to each degree of intensity. It makes reference to vulnerability classes, which are a way to group together buildings characterized by a similar seismic behaviour; six classes (from A to F) of decreasing vulnerability are introduced and, for each of them, the intensity, that can be estimated from a certain damage pattern, is supplied in terms of damage matrices. The damage matrix defined in the EMS-98 scale, which considers 5 damage grades and also the absence of damage, gives the probability that buildings belonging to a certain vulnerability class suffer a certain damage level for a given seismic intensity (see the example given in Table 6.1).

These damage matrices can be used for vulnerability assessments, but the model that they provide is vague and incomplete. The definition for the damage quantification in Table 6.1 is, indeed, provided in a vague way through the quantitative terms “Few”, “Many”, “Most” as the aim is a post-earthquake survey and a precise determination of quantities is not envisaged. Moreover, the distribution of damage is incomplete as the macroseismic scale only considers the most common and easily observable situations

Register for free at <https://www.scipedia.com> to download the version without the watermark

(for example, no information is provided for damage grade 3, 4 and 5 for I = VI and vulnerability class B in Table 6.1).

Table 6.1. Damage model provided by the EMS-98 scale for classes of vulnerability B (Milutinovic and Trendafiloski, 2003; Giovinazzi and Lagomarsino, 2004)

Class B					
Damage level	1	2	3	4	5
Intensity					
V	Few				
VI	Many	Few			
VII		Many	Few		
VIII			Many	Few	
IX				Many	Few
X					Many
XI					Most
XII					

6.3.1.2. The incompleteness problem

In order to solve the incompleteness problem, the damage distributions of earthquakes occurred in the past has been considered; the idea is to complete the EMS-98 model introducing a proper discrete probability distribution of the damage grade. The binomial distribution could be a possibility as it has been successfully used for the statistical analysis of data collected after the 1980 Irpinia earthquake (Italy) (Braga et al. 1983); but the simplicity of this distribution, which depends on only one parameter, does not allow defining the scatter of the damage grades around the mean value.

Sandi and Floricel (1995) observed that the dispersion of the binomial distribution is too high, when you consider a detailed building classification; this may lead to low values of the mean damage grade. The distribution that better suits the specific requirements is the beta distribution (also employed in ATC-13, 1985):

$$PDF : p_{\beta}(x) = \frac{\Gamma(t)}{\Gamma(r)\Gamma(t-r)} \frac{(x-a)^{r-1} (b-x)^{t-r-1}}{(b-a)^{t-1}} \quad a \leq x < b \quad (6.4)$$

$$\mu_x = a + \frac{r}{t} (b-a) \quad (6.5)$$

where a , b , t and r are the parameters of the distribution; μ_x is the mean value of the continuous variable x , which ranges between a and b and $\Gamma(r)$ is the gamma function.

In order to use the beta distribution, it is necessary to make reference to the damage grade D , which is a discrete variable (5 damage grades plus the absence of damage); for this purpose, it is advisable to assign value 0 to the parameter a and value 6 to the parameter b . Starting from this assumption, it is possible to calculate the probability associated with damage grade k ($k=0, 1, 2, 3, 4, 5$) as follows:



$$p_k = P_\beta(k+1) - P_\beta(k) \tag{6.6}$$

Following from this assumption, the mean damage grade, defined as the mean value of the discrete distribution.

$$\mu_D = \sum_{k=0}^5 p_k \cdot k \tag{6.7}$$

and the mean value μ_x (6.5) can be correlated through the following third degree polynomial:

$$\mu_x = 0.042\mu_D^3 - 0.315\mu_D^2 + 1.725\mu_D \tag{6.8}$$

Thus, by using (6.5) and (6.8), it is possible to correlate the two parameters of the beta distribution with the mean damage grade

$$r = t(0.007\mu_D^3 - 0.0525\mu_D^2 + 0.2875\mu_D) \tag{6.9}$$

The parameter t affects the scatter of the distribution; if $t=8$ is used, the beta distribution looks very similar to the binomial distribution.

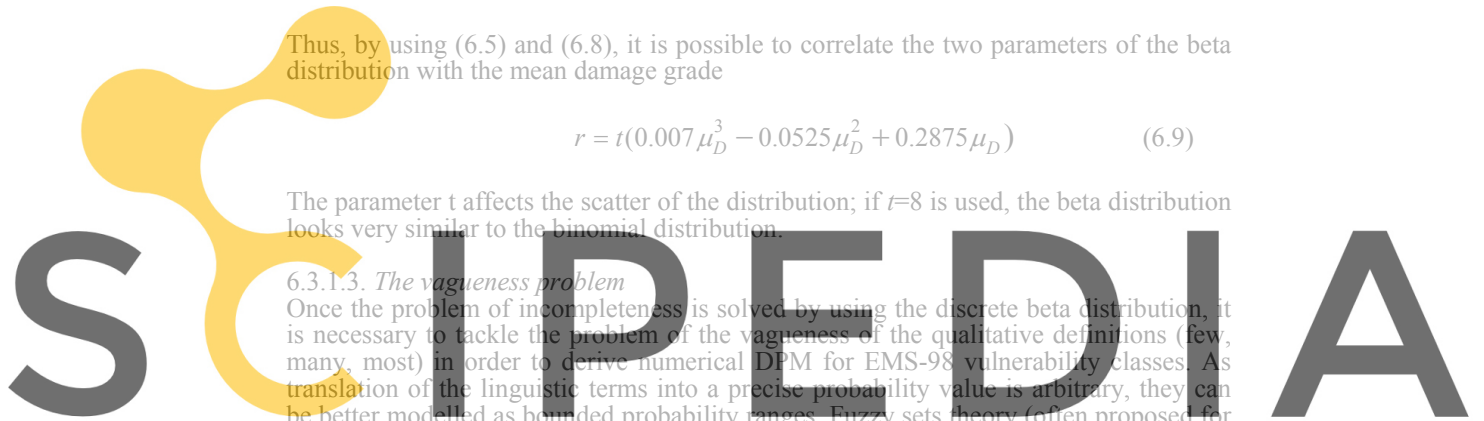
6.3.1.3. The vagueness problem

Once the problem of incompleteness is solved by using the discrete beta distribution, it is necessary to tackle the problem of the vagueness of the qualitative definitions (few, many, most) in order to derive numerical DPM for EMS-98 vulnerability classes. As translation of the linguistic terms into a precise probability value is arbitrary, they can be better modelled as bounded probability ranges. Fuzzy sets theory (often proposed for seismic risk assessment methods) has offered an interesting solution to the problem, leading to the estimation of upper and lower bounds of the expected damage (Benford et al., 1997). According to fuzzy sets theory, the qualitative definitions can be interpreted through membership functions χ , (Dubois and Parade, 1980). A membership function defines the belonging of single values of a certain parameter to a specific set; the value of χ is 1 when the degree of belonging is plausible (that is to say almost sure), while a membership between 0 and 1 indicates that the value of the parameter is rare but possible; if χ is 0, the parameter does not belong to the set.

Figure 6.1 shows the range of percentage of damaged buildings corresponding to the quantitative terms given by the EMS-98. It contends that while there are some definite ranges (few, less than 10%; many, 20% to 50%; most, more than 60%), there are situations of different terms overlapping (between 10% and 20% can be defined as both few and many; 50% and 60%, both many or most). These qualitative definitions are represented through the membership functions χ in Figure 6.1.

6.3.1.4. EMS-98 damage probability matrices

Using fuzzy sets theory and starting from EMS-98 definitions (e.g. Table 6.1), it is possible to build a DPM through the discrete beta distribution (3). Recalling that to each value of parameter μ_D , having definitely assumed $a=0$, $b=6$ and for a fixed value of t , a damage grade distribution corresponds, researchers have looked for μ_D values able to represent the terms “Few”, “Many”, “Most” in a plausible and then in a possible way, according to the membership functions associated to the quantitative definitions. In order to make the operation easier, a value $t=8$ may be used, but it has been verified that



Register for free at <https://www.scipedia.com> to download the version without the watermark

for different values of t , the differences observed are negligible. From the probabilistic distributions corresponding to the computed μ_D values, the percentages of damage have been attributed to the different damage grades. As an example, it is possible to consider the vulnerability class B and the macroseismic intensity VI. Table 6.2 shows for the vulnerability class B, the upper and lower bounds of the mean damage grade related to plausibility and possibility. The corresponding distributions of the damage grades are also shown; the dark and light grey cells correspond to the control definitions and the value that determines the bound is shown as a bold character (Giovinazzi and Lagomarsino, 2004).

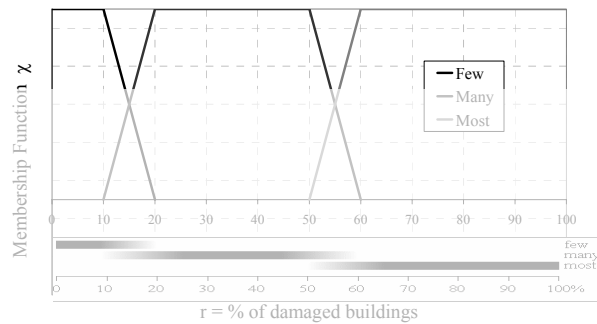


Fig. 6.1. Percentage ranges and membership functions χ of the quantitative terms “Few”, “Many”, “Most”

Table 6.2. Damage distributions and mean damage values related to the upper and lower bounds of plausibility and possibility ranges for vulnerability class B

Class B						
Damage level	1	2	3	4	5	μ_D
Intensity VI	Many	Few				
B ⁺ Upper plausible	32.0	10	1.9	0.2	0.0	0.68
B ⁺⁺ Upper possible	40.6	20	5.5	0.7	0.0	1.81
B ⁻ Lower possible	10	1.6	0.2	0.0	0.0	0.25

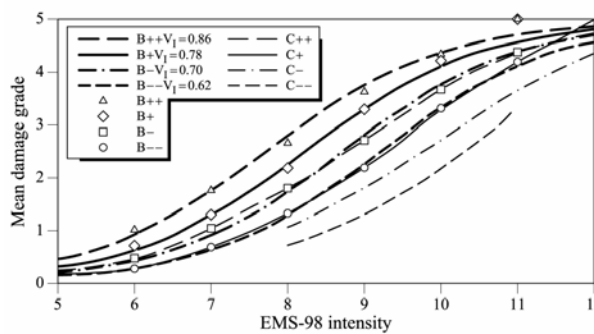
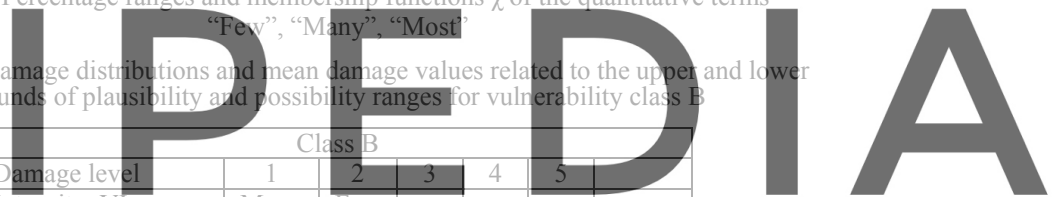


Fig. 6.2. Class B and C plausibility and possibility curves and their interpolation

Repeating this procedure for each vulnerability class and for the different intensity degrees, it is possible to obtain, point by point, the plausible and possible bounds of the mean damage. Connecting these points, draft curves are drawn, which define the



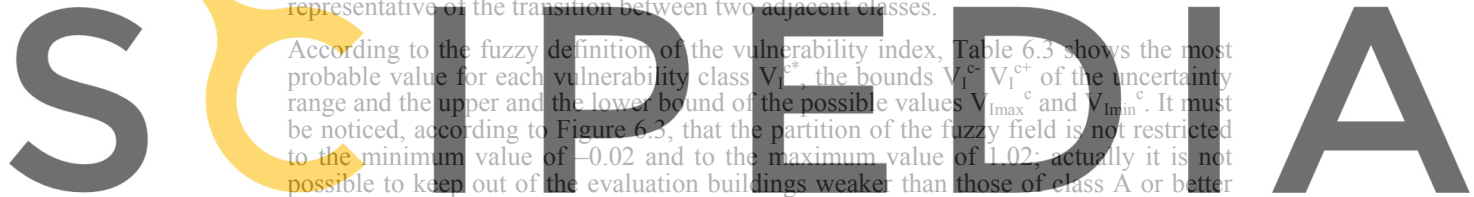
Register for free at <https://www.scipedia.com> to download the version without the watermark

plausibility and possibility areas for each vulnerability class, as a function of the macroseismic intensity (see Figure 6.2).

6.3.1.5. Vulnerability index and vulnerability curves

Observing the curves of Figure 6.2, it stands out that there is a plausible area for each vulnerability class and intermediate possible areas for contiguous classes. In other words, the area between B+ and B- is distinctive for class B, while there is a contiguous area in which the best buildings of class B and the worst of class C coexist (the B- curve coincides with the C++ one; the B-- curve coincides with the C+ one). Another important observation is that curves in Figure 6.2 are, more or less, parallel because the damage produced to buildings of a given vulnerability class by an earthquake of certain intensity, is the same as that caused by an earthquake with the next intensity degree to buildings of the subsequent vulnerability class. On the basis of these considerations, a conventional Vulnerability Index V_1 is introduced within the frame of the fuzzy set theory, indicating that a building pertains to a vulnerability class. The numerical values of the vulnerability index are arbitrary as they are only scores which quantify, in a conventional way, the seismic behavior of a building (they are a measure of the weakness of a building to resist earthquakes). For the sake of simplicity, a 0 to 1 range has been chosen, allowing all possible behaviours to be covered. The values close to 1 correspond to the most vulnerable buildings and the values close to 0 to high-code designed structures. Thus, the membership of a building to a specific vulnerability class can be defined by means of this vulnerability index (see Figure 6.3); in compliance with the fuzzy set theory they have a plausible range ($\chi = 1$) and linear possible ranges, representative of the transition between two adjacent classes.

According to the fuzzy definition of the vulnerability index, Table 6.3 shows the most probable value for each vulnerability class V_1^{c*} , the bounds V_1^{c-} V_1^{c+} of the uncertainty range and the upper and the lower bound of the possible values V_{1max}^c and V_{1min}^c . It must be noticed, according to Figure 6.3, that the partition of the fuzzy field is not restricted to the minimum value of -0.02 and to the maximum value of 1.02; actually it is not possible to keep out of the evaluation buildings weaker than those of class A or better designed than those of class F.



Register for free at <https://www.scipedia.com> to download the version without the watermark

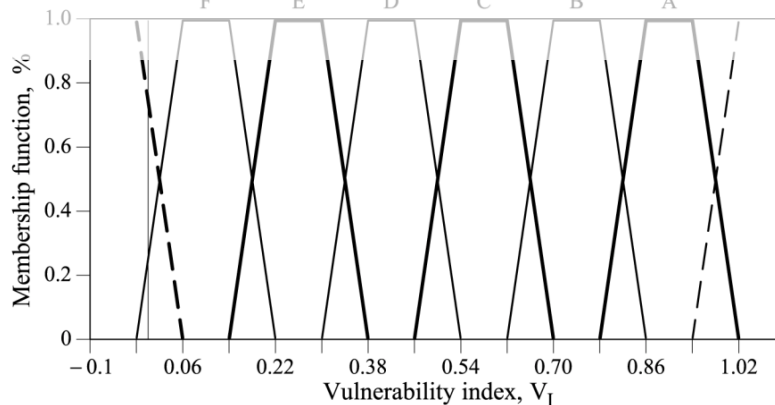


Fig. 6.3. Vulnerability index membership functions for the EMS-98 vulnerability classes

For the operational implementation of the methodology, it is particularly useful to define an analytical expression, capable of describing the curves in Figure 6.2;

therefore, the mean damage grade μ_D is expressed by means of the following function depending on the macroseismic intensity I and the vulnerability index V_I :

$$\mu_D = 2.5 \left[1 + \tanh \left(\frac{I + 6.25 \cdot V_I - 13.1}{2.3} \right) \right] \quad (6.10)$$

Table 6.3. Vulnerability index values for the different vulnerability classes

	$V_{I \min}^c$	V_I^{c-}	V_I^{c*}	V_I^{c+}	$V_{I \max}^c$		$V_{I \min}^c$	V_I^{c-}	V_I^{c*}	V_I^{c+}	$V_{I \max}^c$
A	1.02	0.94	0.9	0.86	0.78	D	0.54	0.46	0.42	0.38	0.3
B	0.86	0.78	0.74	0.7	0.62	E	0.38	0.3	0.26	0.22	0.14
C	0.7	0.62	0.58	0.54	0.46	F	0.22	0.14	0.1	0.06	-1.02

6.3.2. EVALUATION OF THE VULNERABILITY INDEX

The EMS-98 macroseismic scale contains a table with a typological classification of buildings representative for the European countries and vulnerability table (Table 6.4), which distinguishes the buildings as functions of the structural material: masonry, reinforced concrete, steel and timber. Different buildings having the same structural typology are characterized by a prevailing seismic vulnerability class; nevertheless, it is possible to find buildings with a better or worse seismic behavior within the same vulnerability class, depending on their design, constructive or structural characteristics. Therefore, the EMS-98 scale subdivides the seismic behavior of the buildings in six vulnerability classes for which damage probability matrices and vulnerability curves have been evaluated.

The idea highlighted by the EMS-98 scale, according to which the seismic behavior of a building not only depends on the behavior of its structural system but also on other factors, has suggested the following definition of the vulnerability index:

$$\overline{V}_I = V_I^* + \Delta V_R + \Delta V_m \quad (6.11)$$

Register for free at <https://www.scipedia.com> to download the version without the watermark

where ΔV_R and ΔV_m are, respectively, a factor of regional type and of behavior type.

6.3.2.1. Typological vulnerability index

EMS-98 table describes the possibility of a given building typology belonging to a vulnerability class through linguistic terms, as it can be seen in Table 6.4: “Most probable class”, “Possible class”, “Unlikely class”. Even in this case, the fuzzy set theory can provide a useful contribution for the linguistic term interpretation. The belonging of each typology to the vulnerability classes is represented in a fuzzy way, by discriminating the most likely class ($\chi = 1$), the possible class ($\chi = 0.6$) and the unlikely class ($\chi = 0.2$) of Table 6.4. It is possible to define the membership function of each building type as a linear combination of the vulnerability class membership functions, each one considered with its own degree of belonging. As an example, the membership function for massive stone masonry buildings (M4) is shown in Figure 6.4 and it is defined as:

$$\chi_{M4}(V_I) = \chi_C(V_I) + 0.6 \cdot \chi_B(V_I) + 0.2 \cdot \chi_D(V_I) \quad (6.12)$$

where χ_C , χ_B and χ_D are defined in Figure 6.3 (see also Table 6.4.)

From the membership function of each typology, five representative values of V_I have been defined (see Figure 6.4) through a defuzzification process (Ross, 1995): the most probable value of the typological vulnerability index V_I^* for a specific building type is calculated as the centroid of the membership function. V_I^- and V_I^+ , evaluated by a 0.5-

cut of the membership function, are the bounds of the uncertainty range of V_1^* for that building type. V_{1min} and V_{1max} correspond to the upper and lower bounds of the possible values of \bar{V}_1 , that is the final vulnerability index value, for the specific building type. Whatever is the estimated amount of the behavior modifiers and the regional factor, the final vulnerability index has to comply with this possibility range.

Table 6.4. Vulnerability classes of different building typologies (Building Typology Matrix, BTM)

Typologies		Building type	Vulnerability Classes					
			A	B	C	D	E	F
	M1	Rubble stone	■					
	M2	Adobe (earth bricks)	■	■				
	M3	Simple stone	■	■				
	M4	Massive stone		■	■	■		
	M5	Unreinforced M (old bricks)	■	■	■			
	M6	Unreinforced M with r.c. floors		■	■	■		
	M7	Reinforced or confined masonry			■	■	■	
Reinforced Concrete	RC1	Frame in r.c. (without ERD)	■	■	■			
	RC2	Frame in r.c. (moderate ERD)		■	■	■	■	
	RC3	Frame in r.c. (high ERD)			■	■	■	
	RC4	Shear walls (without ERD)		■	■	■		
	RC5	Shear walls (moderate ERD)			■	■	■	
	RC6	Shear walls (high ERD)				■	■	
Steel	S	Steel structures			■	■	■	
Timber	W	Timber structures			■	■	■	

Situations: ■ Most probable class ■ Possible class ■ Unlikely class
 ERD – “Earthquake Resistance Design”

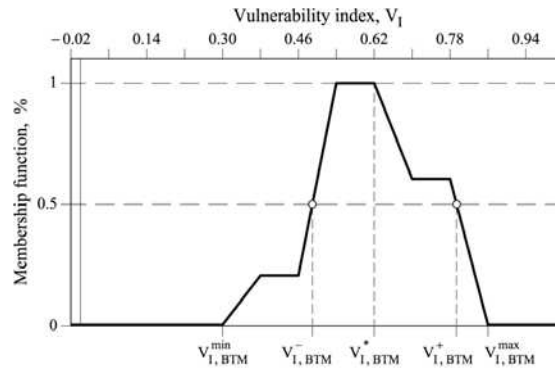


Fig. 6.4. Vulnerability Index membership functions for M4 massive stone typology and \bar{V}_1 values

$$\max(\bar{V}_1; V_{1min}) \leq \bar{V}_1 \leq \min(\bar{V}_1; V_{1max}) \tag{6.13}$$

These values are represented in Figure 6.4 for the massive stone masonry typology and in Table 6.5 for all the EMS-98 buildings typologies.

Table 6.5. Vulnerability index values for the EMS-98 building typologies

Typologies		Building type	Vulnerability classes				
			$V_{I_{min}}$	V_1^-	V_1^+	V_1^+	$V_{I_{max}}$
Masonry	M1	Rubble stone	0.62	0.81	0.873	0.98	1.02
	M2	Adobe (earth bricks)	0.62	0.687	0.84	0.98	1.02
	M3	Simple stone	0.46	0.65	0.74	0.83	1.02
	M4	Massive stone	0.3	0.49	0.616	0.793	0.86
	M5	Unreinforced M (old bricks)	0.46	0.65	0.74	0.83	1.02
	M6	Unreinforced M with r.c. floors	0.3	0.49	0.616	0.79	0.86
	M7	Reinforced or confined masonry	0.14	0.33	0.451	0.633	0.7
Reinforced Concrete	RC1	Frame in r.c. (without ERD)	0.3	0.49	0.644	0.8	1.02
	RC2	Frame in r.c. (moderate ERD)	0.14	0.33	0.484	0.64	0.86
	RC3	Frame in r.c. (high ERD)	-0.02	0.17	0.324	0.48	0.7
	RC4	Shear walls (without ERD)	0.3	0.367	0.544	0.67	0.86
	RC5	Shear walls (moderate ERD)	0.14	0.21	0.384	0.51	0.7
	RC6	Shear walls (high ERD)	-0.02	0.047	0.224	0.35	0.54
Steel	S	Steel structures	-0.02	0.17	0.324	0.48	0.7
Timber	W	Timber structures	0.14	0.207	0.447	0.64	0.86

ERD – “Earthquake Resistance Design”

6.3.2.2. The behaviour modifier factor

The typological vulnerability index V_1^* calculated for each building typology has to be increased or decreased according to the vulnerability recognized for a certain building. The overall score that modifies the characteristic vulnerability index V_1^* can be evaluated, for a single building, simply summing all the modifier scores.

$$\Delta V_m = \sum V_m \quad (6.14)$$

These modifiers are related to the state of preservation of the buildings, the structural system, the height of the building within each building typology, irregularities in plan, elevation and of stiffness, retrofitting interventions, soil morphology and foundation, as well as aggregate building position and elevation (Milutinovic and Trendafiloski, 2003).

If a group of buildings, belonging to a certain typology, is considered, the modifier factor ΔV_m , is evaluated as:

$$\Delta V_m = \sum_k r_k \cdot V_{m,k} \quad (6.15)$$

where r_k is the ratio of building affected by the behaviour modifier k characterized by a $V_{m,k}$ score. Making reference to single buildings, the behaviour modifier factor ΔV_m is simply the sum of the scores $V_{m,k}$ for the recognized behaviour modifiers. The identification of the behavior modifiers can be made empirically, based on the observation of typical damage pattern and taking also into account the suggestions made in several inspection forms (ATC-21, 1988; Benedetti and Petrini, 1984; UNDP/UNIDO, 1985) and by previous proposals (Coburn and Spence, 2002). The modifying scores V_m can be also assigned using expert judgment followed by a partial calibration by comparison with other vulnerability evaluations; but a better calibration is desirable on the basis of damage and vulnerability data collected after earthquakes. Giovinazzi and Lagomarsino (2004) propose behaviour modifier factors and the corresponding scores for masonry and reinforced concrete buildings.

6.3.2.3. *The regional vulnerability factor*

The range bounded by V_1^- , V_1^+ is quite large in order to be representative for the huge variety of the constructive techniques used all around the different countries. The regional vulnerability factor takes into account the characteristics of the buildings belonging to a certain typology at regional level: a major or minor vulnerability could be indeed recognized due to some traditional constructive techniques used in the region.

According to this regional vulnerability factor the V_1^* typological vulnerability index is modified on the basis of an expert judgment or on the basis of the historical data available. The first case is achieved when precise technological, structural and constructive information is available, attesting an effective better or worse average behavior with regard to the one proposed in Table 6.5. The second one occurs when observed damages data are available; the average curve ($\bar{V}_1 = V_1^*$ in Equation 6.11) can be shifted in order to obtain a better approximation for the same data.

6.3.2.4. *Uncertainty range in the vulnerability assessment*

The uncertainties affecting a seismic risk analysis are both epistemic and random. The epistemic ones refer in this case to uncertainties associated with the classification of the exposed building stock into a vulnerability class or into a building typology and by the uncertainties associated with the assignment of a characteristic behaviour to the vulnerability class or building typology (Spence et al., 2003). Considering both kinds of uncertainties allows obtaining the most probable vulnerability index as well as its plausibility and possibility ranges for each vulnerability class (Table 6.3) and for each building typology (Table 6.5).

It must be noticed that the uncertainty affecting building typologies is higher than the one affecting vulnerability classes because the building typology behaviour has been deduced from the one observed from vulnerability classes and, furthermore, because with few data it is more difficult to classify a building into a typology rather than into a vulnerability class. But the knowledge of information additional to the typological one, limits the uncertainties of the building behavior; it is therefore advisable not only to modify the most probable value V_1^* (according to Equation 6.11), but also to reduce the range of its uncertainty ($V_1^- \div V_1^+$). This goal is achieved by modifying the membership function through a filter function f , centered in the new most probable value \bar{V}_1 , depending on the parameter ΔV_f , representing the width of the filter function (Giovinazzi and Lagomarsino, 2004).

6.3.2.5. *Example*

The city of Barcelona, Spain, is located in an area of low to moderate seismic hazard, but its buildings show a high vulnerability and, consequently, a significant probability of being damaged even in the case of a not excessively severe earthquake. The total number of dwellings of Barcelona is about 700.000, with an average of 2.2 inhabitants in each, and about 63.000 buildings. The majority of Barcelona's most representative unreinforced masonry buildings, with an average age of 60 years, were designed only considering vertical static loads, without any seismic design criteria, greatly influencing the overall seismic vulnerability of the city. Additionally, some of its particular features, typical for the constructive techniques of the city at that time, have been identified as potential damage sources. The slabs of these unreinforced masonry buildings are made of wood, steel or reinforced concrete, according to the building period, and have ceramic ceiling vaults in all the cases. Due to the higher height of the first floor, almost all of these buildings have soft first floors. In many cases, cast iron columns were used

instead of masonry walls at the base and ground floors, reducing thus even more their stiffness. The majority of the reinforced concrete buildings of Barcelona have waffle slabs, a structural member not adequate for seismic areas. Many of the buildings in Barcelona are part of aggregates.

Traditionally, the vulnerability index method identifies the existing building typologies within the studied area and defines their vulnerability class (Table 6.4). For each vulnerability class, the relationship between intensity and damage may be defined by using Damage Probability Matrices. The specific buildings of Barcelona are classified in different groups characterized by a similar seismic behaviour. All the buildings belonging to each typology are cast within the most probable class.

Table 6.6. Vulnerability index for typologies and periods of construction of Barcelona, according to the seismic design level

Periods	Period of construction	Spanish Code	Obligation in Barcelona	Lateral bracing in constructive practice	Seismic Design level	Buildings (%)	Vulnerability Index (V_i)			
							M31 M32 M33	M34	RC32	
I	<1950	----	----	Absent	Pre-code	50.69	0.938	--	--	
II	1950-1962	----	----	Deficient	Pre-code	17.30	0.875	--	--	
III	1963-1968	Recommendation MV-101 (1962)	No specified	Deficient	Pre-code	10.91	0.813	0.750	0.750	
IV	1969-1974	Seismic code P.G.S.-1 (1968)	Yes	Acceptable	Low-code	9.80	0.750	0.625	0.625	
V	1975-1994	Seismic code P.D.S. (1974)	Yes	Acceptable	Low-code	11.07	0.688	0.563	0.500	
VI	1995 until now	Seismic code NCSE-94 (1995)	No	Acceptable	Low-code	0.23	0.688	0.563	0.500	

Figure 6.5 shows vulnerability maps for both the unreinforced masonry and reinforced concrete buildings of Barcelona

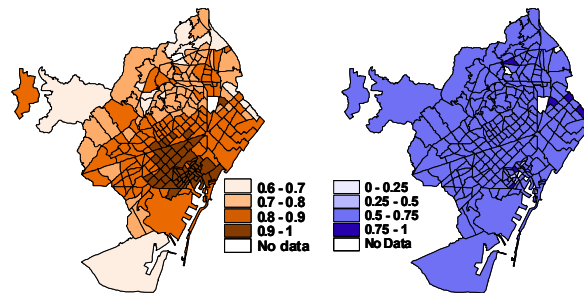


Fig. 6.5. Vulnerability indices maps for unreinforced masonry buildings (left) and reinforced concrete buildings (right)

Vulnerability indices are assigned to the most representative building typologies of Barcelona, representing scores that quantify their seismic behaviour. A first refinement of this average initial vulnerability index is performed by taking into account the age of the building. The building stock is grouped in 6 age categories by considering reasonable time periods as functions of the existence of seismic codes in Spain and its

level, as well as other specific construction features (see Table 6.6) (Lantada et al., 2004).

The global vulnerability index of each building is now evaluated by applying behaviour modifiers (Equation 6.14), which are different for isolated and aggregate buildings. For isolated buildings, the following 4 modifiers were considered: number of floors, irregularity in height, length of the façade and state of preservation. For building in aggregates the effects due to the different heights of adjacent buildings and the effects due to the position of the building in the aggregate (i.e. corner, header, or intermediate) have been taken into account.

6.4. Capacity spectrum method

The capacity spectrum method uses the capacity and demand spectra to obtain the performance point of the structure which corresponds to its maximum spectral displacement, and uses fragility curves to obtain the damage probability for the expected seismic input. Capacity curves are force-displacement diagrams of the structure which correspond to the first mode maximum response of buildings and governing the structural damage; they mainly depend on the structural design and construction practice. The performance of a building is directly influenced by the level and frequency content of the seismic action which controls the peak building response levels. The seismic input is modelled by means of the demand spectrum, which is the inelastic structural response spectrum. This demand spectrum can be obtained by using a nonlinear structural analysis or, in a simplified way, starting from the 5% damped building-site specific elastic response spectrum modified to account for the inelastic structural behaviour. Both the capacity and demand spectra are represented in the spectral acceleration (Sa)-Spectral displacement (Sd) domain.

Fragility curves define the probability that the expected damage d exceeds a given damage state d_s , as a function of a parameter quantifying the severity of the seismic action. Thus, fragility curves are completely defined by plotting $P(d \geq d_s)$ in ordinate and the spectral displacement Sd in abscissa. If it is assumed that fragility curves follow a lognormal probability distribution, they can be completely defined by only two parameters which, in this case, are the mean spectral displacement \overline{Sd}_{d_s} and the corresponding standard deviation β_{d_s} .

Fragility curves can be obtained in a simplified way starting from the bilinear representation of capacity curves (see Figure 6.6 and Table 6.7). Crossing demand and capacity spectra, the performance point is established and thus the expected spectral displacement which, together with the corresponding fragility curves, allows obtaining probability matrices for the damage scenario corresponding to earthquakes defined by their demand spectra. Therefore, all the fragility and damage analyses are based in a straightforward manner on capacity and demand spectra and fragility curves.

The method for analyzing the seismic damage considers 5 damage states: none, slight, moderate, extensive and complete. For a given damage state, a fragility curve is well described by the following lognormal probability density function:

$$P[d_s / Sd] = \Phi \left[\frac{1}{\beta_{d_s}} \ln \left(\frac{Sd}{\overline{Sd}_{d_s}} \right) \right] \quad (6.16)$$

where \overline{Sd}_{ds} is the threshold spectral displacement at which the probability of the damage state d_s is 50%, β_{ds} is the standard deviation of the natural logarithm of this spectral displacement, Φ is the standard normal cumulative distribution function and Sd is the spectral displacement. Figure 6.6 and Table 6.7 show how the \overline{Sd}_{ds} thresholds are obtained from the capacity spectra. Concerning β_{ds} , it is well known that the expected seismic damage in buildings follows a binomial probability distribution. Therefore, it is assumed that at the \overline{Sd}_{ds} threshold, the probability of this damage state is 50% and then the probabilities of the remaining damage states are estimated.

Starting from the spectral displacement corresponding to the performance point, damage probability matrices can be obtained by using the corresponding fragility curves. A weighted average damage index, DS_m , can be calculated by using the following equation:

$$DS_m = \sum_{i=0}^4 DS_i P[DS_i] \quad (6.17)$$

where DS_i takes the values 0, 1, 2, 3 and 4 for the damage states i considered in the analysis and $P[DS_i]$ are the corresponding probabilities.

Table 6.7. Damage state thresholds defined in agreement with the capacity spectrum

$\overline{Sd}_1 = 0.7D_y$	Slight
$\overline{Sd}_2 = D_y$	Moderate
$\overline{Sd}_3 = D_y + 0.25(D_u - D_y)$	Extensive
$\overline{Sd}_4 = D_u$	Complete

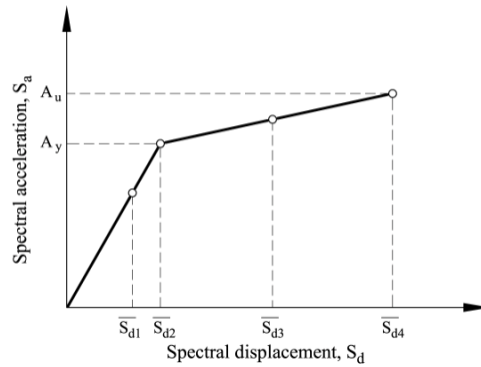


Fig. 6.6. Damage state thresholds from capacity spectrum

It can be considered that DS_m is close to the most likely damage state of the structure. According to Equation 6.17, a value $DS_m=1.3$, for example, indicates that the most probable damage state of a building ranges between *slight* and *moderate*, being more probable the *slight* damage state. This average damage index permits plotting seismic damage scenarios by using a single parameter. Of course, alternative maps may plot the

spatial distribution of the probability of occurrence of a specific damage state, that is $P[DS_i]$.

6.4.1. EXAMPLE

For illustration of the method we use the same example of Barcelona which has a moderate seismicity and weak tectonic motions; its seismic hazard has been recently re-evaluated defining the action in terms of elastic response acceleration spectra both from a deterministic and a probabilistic approach (Irizarry et al., 2003). Two earthquake scenarios have been developed and used to perform the simulations of seismic risk scenarios, one deterministic, based on a historical earthquake that occurred quite far from the city and whose intensity at the basement and outcrop has been estimated, and the other probabilistic, corresponding to a 475 years return period. The result of both simulations can be seen in Figure 6.7 in acceleration-displacement format (ADRS). The same figure shows a seismic risk scenario in macroseismic intensities, used to develop seismic risk scenarios according to the vulnerability index method.

Detailed structural plans have been used to model representative buildings for low-rise (two stories, 5.2 m high) mid-rise (five stories, 15.8 m high) and high-rise (eight stories, 24.0 m high) reinforced concrete buildings. Capacity curves were obtained by performing non-linear static analyses using RUAUMOKO-2D program (Carr, 2000). In a similar way, based on detailed structural plans, two stories (low-rise), four stories (mid-rise) and six stories (high-rise) buildings of the Eixample district of Barcelona have been modelled. TreMuri program (Galasco et al., 2002) was used to perform the dynamic analyses of the buildings. Pushover analyses allowed obtaining the capacity curves for each building class. Table 6.8 shows the yield and ultimate capacity points defining the bilinear capacity spectra for reinforced concrete and masonry buildings. It can be seen how the capacity decreases with the height of the building both for masonry and for RC buildings.

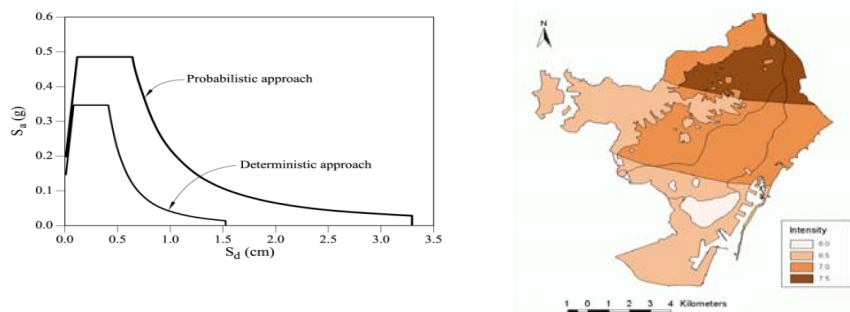


Fig. 6.7. Response spectra for deterministic and probabilistic hazard scenarios (left) and deterministic seismic hazard scenario including local soil effects in intensity (right) (Irizarry et al., 2003)

Table 6.9 shows the expected probabilities of all the damage states when a particular damage state probability is fixed to 50% and a binomial or equivalent beta probability distribution is assumed. In this table, the damage states are represented by numbers from 1 to 4 for damage states *slight* to *complete*, respectively. The probabilities in this table are cumulative and correspond to the points shown in Figure 6.8. Parameter DS_m controls the assumed probability distribution. Finally, the function expressed by Equation 6.16 is fitted to the obtained points by means of a least square criterion.

Table 6.8. Yield and ultimate capacity for reinforced concrete (RC) and masonry (M) buildings

Building class	Yield capacity		Ultimate capacity	
	Dy (cm)	Ay (g)	Du (cm)	Au (g)
Low-rise, RC	0.70	0.129	5.240	0.138
Mid-rise, RC	1.418	0.083	5.107	0.117
High-rise, RC	1.894	0.059	4.675	0.079
Low-rise, M	0.27	0.651	1.36	0.558
Mid-rise, M	0.63	0.133	2.91	0.117
High-rise, M	0.68	0.105	2.61	0.079

Table 6.9. Probabilities of the expected damage states when fixing a 50% probability for each damage state: 1-slight, 2-moderate, 3-extensive and 4-complete

Condition	DS_m	$P_\beta(1)$	$P_\beta(2)$	$P_\beta(3)$	$P_\beta(4)$
$P_\beta(1)=0.5$	0.911	0.500	0.119	0.012	0.00
$P_\beta(2)=0.5$	1.919	0.896	0.500	0.135	0.008
$P_\beta(3)=0.5$	3.081	0.992	0.866	0.500	0.104
$P_\beta(4)=0.5$	4.089	1.000	0.988	0.881	0.500

Figure 6.8 shows an example of such a fit. Points in this figure correspond to the damage state probabilities and lines are the fitted fragility curves. This figure corresponds to the mid-rise reinforced concrete building class. Table 6.10 shows the corresponding parameters, namely \bar{Sd}_i and β_i , where $i=1, \dots, 4$ defines the fragility curves corresponding to reinforced concrete (RC) and unreinforced masonry (M) building classes. The demand spectra, together with the capacity spectra have been used to obtain the performance point which defines the maximum expected spectral displacement related to a specific demand. Entering in the fragility curves with the spectral displacement of the performance point, the structural damage probabilities are established and seismic risk scenarios can be then obtained.

Table 6.10. Parameters characterizing the fragility curves, for reinforced concrete buildings (RC) and unreinforced masonry buildings (M)

Building class	Damage states thresholds							
	\bar{Sd}_1 (cm)	β_1	\bar{Sd}_2 (cm)	β_2	\bar{Sd}_3 (cm)	β_3	\bar{Sd}_4 (cm)	β_4
Low-rise, RC	0.49	0.28	0.70	0.37	1.84	0.82	5.24	0.83
Mid-rise, RC	0.99	0.28	1.42	0.36	2.34	0.50	5.11	0.61
High-rise, RC	1.33	0.28	1.89	0.29	2.59	0.34	4.68	0.45
Low-rise, M	0.19	0.28	0.27	0.37	0.54	0.54	1.36	0.72
Mid-rise, M	0.44	0.40	0.63	0.50	1.20	0.75	2.91	0.70
High-rise, M	0.46	0.30	0.68	0.65	1.68	0.65	2.61	0.65

The response spectra for the deterministic and probabilistic hazard scenarios (Figure 6.7), together with the capacity curves described in Table 6.8, allowed obtaining the

performance point and, using the corresponding fragility curves of Table 6.9 and the damage probability matrices of Table 6.10.

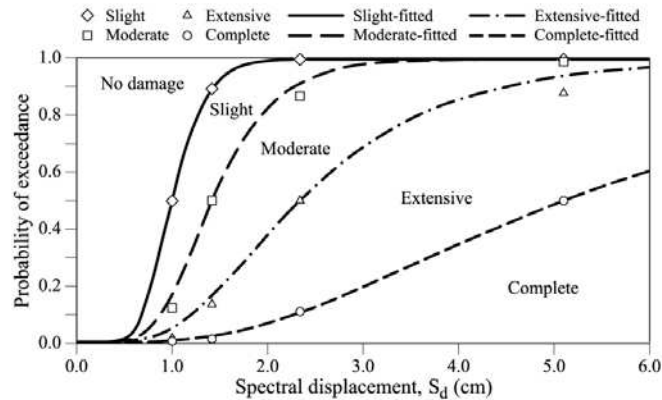


Fig. 6.8. Fragility curves for mid-rise reinforced concrete buildings

6.5. Final remarks

Both the vulnerability index and capacity spectrum methods provide excellent results, showing an excellent correlation with the main features of the built-up environment of Barcelona. It is clear in both cases that a city located in a low to moderate hazard region has paid no attention to the seismic performance of their buildings, and therefore, a high seismic vulnerability and a considerable risk are expected.

Another interesting feature of the described methodologies is their ability to draw the main characteristics of the built-up environment of the city, underlying the radial pattern of the damage. Downtown, where population density is higher and economy is more active, we find the highest vulnerability. The methods described here may be easily adapted to outline risk evaluations for other cities. Probably most of the vulnerability indices adopted for Barcelona may be slightly modified and directly used for obtaining risk scenarios for other cities of Spain and, in particular, for those situated in the Mediterranean region.

Acknowledgements

This work has been partially sponsored by the Spanish Ministry of Science and Technology and with FEDER funds (projects: REN 2001-2418-C04-01 and REN2002-03365/RIES) and by the European Commission (RISK-UE Project: "An advanced approach to earthquake risk scenarios with applications to different European towns", contract EVK4-CT-2000-00014).